

Direct laser writing of flexible graphene field emitters

Georgios Viskadourous, Dimitrios Konios, Emmanuel Kymakis, and Emmanuel Stratakis

Citation: [Applied Physics Letters](#) **105**, 203104 (2014); doi: 10.1063/1.4902130

View online: <http://dx.doi.org/10.1063/1.4902130>

View Table of Contents: <http://scitation.aip.org/content/aip/journal/apl/105/20?ver=pdfcov>

Published by the [AIP Publishing](#)

Articles you may be interested in

[Solid-state fabrication of ultrathin freestanding carbon nanotube–graphene hybrid structures for field emission applications](#)

J. Vac. Sci. Technol. B **32**, 06FF03 (2014); 10.1116/1.4899241

[Transparent, flexible, and solid-state supercapacitors based on graphene electrodes](#)

APL Mat. **1**, 012101 (2013); 10.1063/1.4808242

[Multi-finger flexible graphene field effect transistors with high bendability](#)

Appl. Phys. Lett. **101**, 252109 (2012); 10.1063/1.4772541

[Effective large-area free-standing graphene field emitters by electrophoretic deposition](#)

Appl. Phys. Lett. **101**, 183107 (2012); 10.1063/1.4765070

[Flexible field emitter arrays with adjustable carbon nanotube distances and bundle generation](#)

J. Vac. Sci. Technol. B **28**, 268 (2010); 10.1116/1.3298889



Direct laser writing of flexible graphene field emitters

Georgios Viskadourous,^{1,2} Dimitrios Konios,¹ Emmanuel Kymakis,^{1,a)}
 and Emmanuel Stratakis^{1,3,4,a)}

¹Center of Materials Technology and Photonics and Electrical Engineering Department,
 Technological Educational Institute (TEI) of Crete, Heraklion 71004, Crete, Greece

²Department of Mineral Resources Engineering, Technical University of Crete, Chania 731 00, Crete, Greece

³Institute of Electronic Structure and Laser, Foundation for Research and Technology - Hellas,
 P. O. Box 1527, 711 10 Heraklion, Crete, Greece

⁴Department of Materials Science and Technology, University of Crete, Heraklion 710 03, Crete, Greece

(Received 15 October 2014; accepted 8 November 2014; published online 19 November 2014)

We report on the simple fabrication of highly efficient solution-processable, flexible graphene-based field emission (FE) cathodes via direct laser writing of emitting pixels on reduced graphene oxide (rGO) films deposited onto rGO:poly(3-hexylthiophene) (P3HT) composite layers. Laser processing gives rise to a pronounced vertical alignment of rGO bundles perpendicular to the substrate, while at the same time sharp graphene edges are protruding out of the bundle. The laser-fabricated cathodes exhibit outstanding FE properties with a turn-on field of as low as $\sim 0.6 \text{ V}/\mu\text{m}$ and a field enhancement factor of 8900, which are the best reported to date for rGO FE cathodes. At the same time, the cathodes exhibit stable operation under extensive and repetitive bending, a critical requirement for every flexible technology. The flexible and solution-processable, graphene-based, technology developed could be useful for diverse potential applications including field emission displays, biochemical sensors as well as solar cell and battery electrodes. © 2014 AIP Publishing LLC.

[<http://dx.doi.org/10.1063/1.4902130>]

Flexible electronics¹ have been a growing part of research and development in organic electronics due to their expanding applications, including touch screens, optical displays, e-paper, photovoltaics, lighting devices, and sensors.^{2–5} This technology is based on the controlled deposition and/or printing of different solution-processed layers that form the various device components, onto mechanically flexible substrates. A critical requirement for this technology is that the fabrication processes must be compatible with the nominally low-temperature plastic materials that are being considered for the substrates. In addition to the electrical and optical properties, the ideal solution-processable electronic material should be mechanically robust under extensive bending.

Field emission (FE) refers to a quantum mechanical tunneling phenomenon where high-density electrons are emitted from a sharpened cathode tip under the action of a strong electric field. This simple principle is widely utilized in many applications including electron guns,⁶ microwave power amplifiers,⁷ X-ray tubes,⁸ neutralizers for space propulsion devices,⁹ electron beam lithography,¹⁰ and large-area field emission sources such as flat panel field emission displays (FEDs).¹¹ Nevertheless, the successful integration of FE into flexible device architecture remains a technological challenge due to the high-performance requirements of FE materials including high FE current as well as electrical and mechanical robustness in an extremely deformed geometry. In this respect, graphene is promising candidate, owing to its intrinsic flexibility and stretchability, as well as excellent electrical properties.¹² More importantly, due to its

inherent 2D geometry, graphene should give rise to high geometric field enhancement, allowing the extraction of electrons at low threshold electric fields.¹³

However, due to the poor solubility and yield of micro-mechanically cleaved graphene, solution-processed graphene derivatives have been synthesized to be used in flexible electronic devices. Among various candidates, reduced graphene oxide (rGO) produced by exfoliation of graphite oxide in solution¹⁴ and subsequent reduction,¹⁵ appears to be the most straightforward approach to obtain a solution processable and highly conductive graphene. In addition to this, it has been shown that the presence of edge functional groups in rGO sheets periphery substantially lower the work function, facilitating easier tunneling of electrons compared to graphene.¹⁶ Accordingly, highly efficient rGO-based FE can be realized provided that atomic thin edges are exposed to electric field, and for this purpose graphene sheets need to be aligned perpendicular on conducting substrates. So far, a number of rGO-based flexible FE cathodes have been realised, including hybrid carbon nanotube(CNT)-rGO films,^{17,18} nanowire-rGO nanostructures.¹⁹ In all cases, however, deposition of rGO from solution typically leads to rGO sheets that lay flat on the substrate surface or protruding at small angles from the substrate, thus limiting the geometrical field enhancement. More importantly, in all these cases rGO sheets did not function as the primary emitting material. In this respect, the realisation of flexible FE cathodes comprising perpendicularly oriented rGO sheets remains a critical challenge.

In this letter, we present a methodology to fabricate highly efficient flexible graphene-based FE cathodes based on drop-casting of rGO on composite rGO:P3HT polymer layers and subsequent direct laser texturing; direct laser

^{a)}Authors to whom correspondence should be addressed. Electronic addresses: kymakis@staff.teicrete.gr and stratak@iesl.forth.gr.

writing (DLW) has emerged as a promising technique for the rapid and facile fabrication of graphene for various applications.²⁰ It is shown that proper laser treatment gives rise to preferential protrusion of rGO sheets from the substrate and in series to FE characteristics superior to those of pristine rGO. Besides this, the performance of the developed flexible cathodes is preserved upon extensive bending conditions. The proposed fabrication method can potentially be a promising solution for superior graphene flexible FE cathodes.

GO was prepared from purified natural graphite powder (Alfa Aesar, ~200 mesh) according to a modified Hummers' method.²¹ For the production of rGO, 40 mg of GO was dispersed in 15 ml of acetic acid and sonicated for 30 min. HI (0.8 ml) was then added and the mixture was stored at 40 °C for 40 h with constant stirring. The product was isolated by filtration, washed with saturated sodium bicarbonate (3 × 3 ml), distilled water (3 × 3 ml) and acetone (2 × 2 ml) and then vacuum dried overnight at room temperature to yield rGO powder. Both rGO and P3HT were dissolved in tetrahydrofuran and sonicated to form homogeneous dispersions of 10 mg/ml concentrations. Composite dispersions were prepared by mixing adequate amounts of the two separate solutions corresponding to rGO loadings, defined as the [rGO/(rGO + P3HT)] volume ratios equal to 10%, 20%, 30%, 60%, and 80%, respectively. The dispersions were then drop casted on the flexible substrate to form uniform composite films. The final cathodes were prepared via drop casting a portion of rGO solution on a previously dried rGO:P3HT composite on PET/ITO and were left to dry at room temperature; the ITO substrate is used to mediate the electrical contact with the field emission equipment. It is observed that the THF in the rGO solution dissolves the polymer on the surface of the composite, allowing integration of the two layers, while leaving the rGO sheets on the surface.

Figure 1(a) shows field emission scanning electron microscopy (FESEM) images of rGO layers drop-casted on rGO:P3HT. It is evident that the rGO flakes were uniformly lay flat onto the substrate, while the sheets comprise sharp edges, sporadically protruding out of the surface. We first studied the influence of rGO:P3HT ratio of the composite substrate on the FE performance by measuring the FE current–voltage (*I*-*U*) characteristics of the five different rGO cathodes prepared. FE measurements were performed under 5×10^{-6} mbar vacuum, using the samples as cold cathode emitters in a planar diode system with a sample-to-anode distance, *d*, equal to $d = 200 \mu\text{m}$. Details for the setup can be found elsewhere.^{22,23} Figure 1(b) shows, on a log-log plot, the current density, *J*, measured as a function of the electric field, *E* for the composite layers of different rGO:P3HT ratios; while, Table I summarizes the turn-on field, *F*_{to}, for different rGO cathodes, defined as the average macroscopic field needed to extract 25 pA/cm². Three distinct regions are always visible in the *J*-*E* data: zero emission, field emission, and current saturation. The observed saturation at high fields and thus the appearance of a knee point in *J*-*E* plots can be attributed to either joule heating, adsorption-related, or high contact resistance effects. In particular, a similar saturation effect was observed in CNT-based emitters and attributed to thermal induced FE that gave rise to blackbody radiation

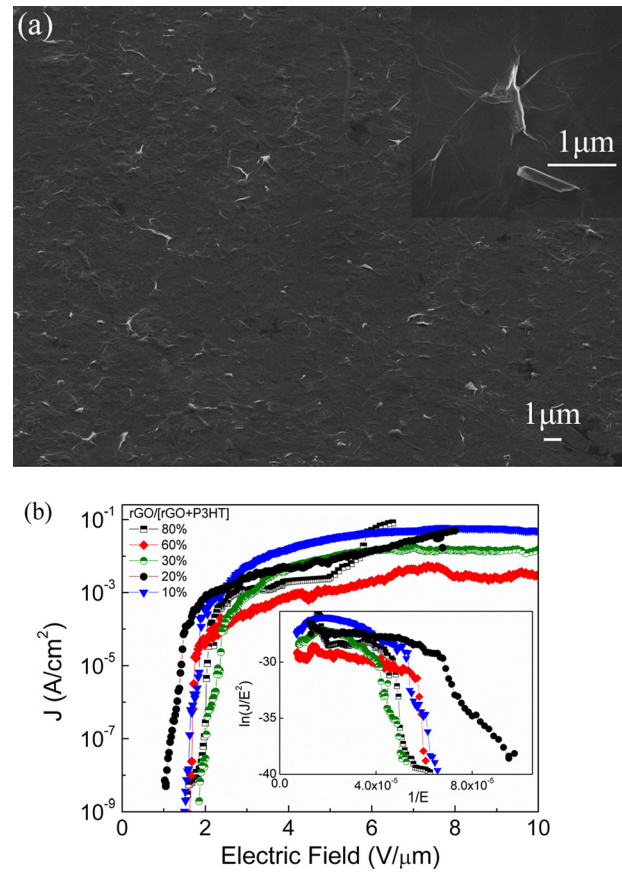


FIG. 1. (a) Typical FESEM view of an rGO layer drop-casted onto a composite rGO:P3HT film deposited on a flexible ITO/PET substrate. The inset presents a high magnification image of a sharp graphene edge; (b) Logarithmic plot of current density-field (*J*-*E*) emission characteristics of rGO layers deposited onto composite rGO:P3HT films with different rGO/(rGO + P3HT) content ratios. The inset presents the respective Fowler-Nordheim plots.

emission.²⁴ Alternatively, other reports attributed noticeable slope changes in the *J*-*E* plots to adsorbents on the emitter tip²⁵ and to a large voltage drop along the emitter and/or at the emitter/substrate interface.^{26,27} Further experiments are currently in progress in order to identify which of the above *J*-*E* curves.

We analyze the *J*-*E* data using the classic theory of Fowler-Nordheim (FN), about field-assisted tunneling process²⁸ in which the current density, *J*, depends on the local microscopic field at the emitter, *E*_{loc}, according to the relationship

$$J = AE_{loc}^2 \exp\left(-\frac{b_{FN}}{E_{loc}}\right), \quad (1)$$

where *A* is a constant that depends on the actual emitting surface structure $b_{FN} = 0.94 \cdot B \cdot \Phi^{3/2}$ with $B = 6.83 \times 10^7 \text{ V cm}^{-1} \text{ eV}^{-3/2}$, and Φ is the work function of the material in eV (assuming that $\Phi = 5.0 \text{ eV}$ for rGO²⁹). *E*_{loc} is usually related to the average macroscopic field, *E*, as follows:

$$E_{loc} = \beta E = \beta \frac{U}{d}, \quad (2)$$

where β is the field enhancement factor. The field enhancement factor values for the different rGO cathodes tested can

TABLE I. Field emission properties of rGO layers with different rGO/(rGO + P3HT) content ratios. The \pm values denote the standard deviation of each measured or estimated quantity.

rGO/(rGO + P3HT) content ratio (vol. %)	10	20	30	60	80	100
Turn-on field, F_{to} (V/ μ m)	1.5 ± 0.1	1.0 ± 0.1	1.9 ± 0.1	1.6 ± 0.1	1.6 ± 0.1	2.2 ± 0.1
Threshold field, F_{th} (V/ μ m)	1.8 ± 0.1	1.4 ± 0.1	2.3 ± 0.1	1.8 ± 0.2	2.0 ± 0.1	2.1 ± 0.1
Field enhancement, β	915 ± 54	2507 ± 112	971 ± 80	290 ± 22	662 ± 41	395 ± 27

be calculated from the respective FN plots, via fitting the linear part of the data at low voltages (Figure 1(b)-inset), following Eq. (1), and are listed in Table I. As also presented in our previous report,²² the best rGO field emitters are those deposited on composite films with relatively low rGO:P3HT ratios (20%). The difference can be attributed to the sheets preferential orientation at different angles relative to the planar substrate as a result of the effect of the polymer, giving rise to a variation of the number of active emitters with polymer loading.²² Alternatively, the FE performance improvement can be attributed to the existence of a triple junction between the conductive substrate, the layer of rGO:P3HT, and vacuum.^{22,30} As shown in Table I, the FE performance of rGO layers on neat PET/ITO was also measured and is found by far inferior to those deposited on composite substrates.

To further enhance the FE performance of the fabricated cathodes, the rGO layers were eventually processed via DLW (Figure 2(a)). The aim was to partially texture the rGO layers and in this way to increase the density of graphene edges exposed to vacuum. The primary advantage of utilizing laser irradiation for texturing lies in the ability for *in-situ* controlled epidermal treatment without practically affecting the integrity of the thermally sensitive substrate underneath. The irradiation experiments were performed using a 170 fs Yb-doped Potassium-Gadolinium Tungstate crystal laser system operating at 1030 nm wavelength and 60 kHz

repetition rate. The laser beam was focused down to $\sim 100 \mu\text{m}$ on the sample, placed on an XY translation stage, at normal incidence. We initially investigated a single-pulse light flux threshold at which the top rGO layer is textured, without practically affecting the composite film and the underlying flexible substrate. Figure 2(b) presents a typical SEM image of a laser-formed spot on the rGO layer surface and its internal texture, respectively, obtained upon irradiation at the threshold fluence of 50 mJ/cm^2 . It is evident that the surface morphology of drop-casted rGO was changed drastically after laser irradiation. In particular, due to the laser texturing effect, graphene flakes tend to be oriented perpendicular to the substrate surface, while at the same time entangled bundles of graphene sheets were raveled out. Besides this, it is observed that the areal density of sharp graphene edges protruding out of the bundle was substantially increased compared to the initial layer surface. For the cathode fabrication DLW of a regular array of spots was performed via scanning the laser beam on the surface. The array of Figure 2(c) comprising spots of vertically oriented rGO sheets (V-rGO) is an alternative approach to the fabrication of functional graphene cold cathodes based on the selective fabrication of spots of field emitters rather than a large continuous emitting area. This process is faster and very effective, since no rastering of the beam across the whole substrate is required. It is also closer to the requirements of the field emission device industry, since each one of these

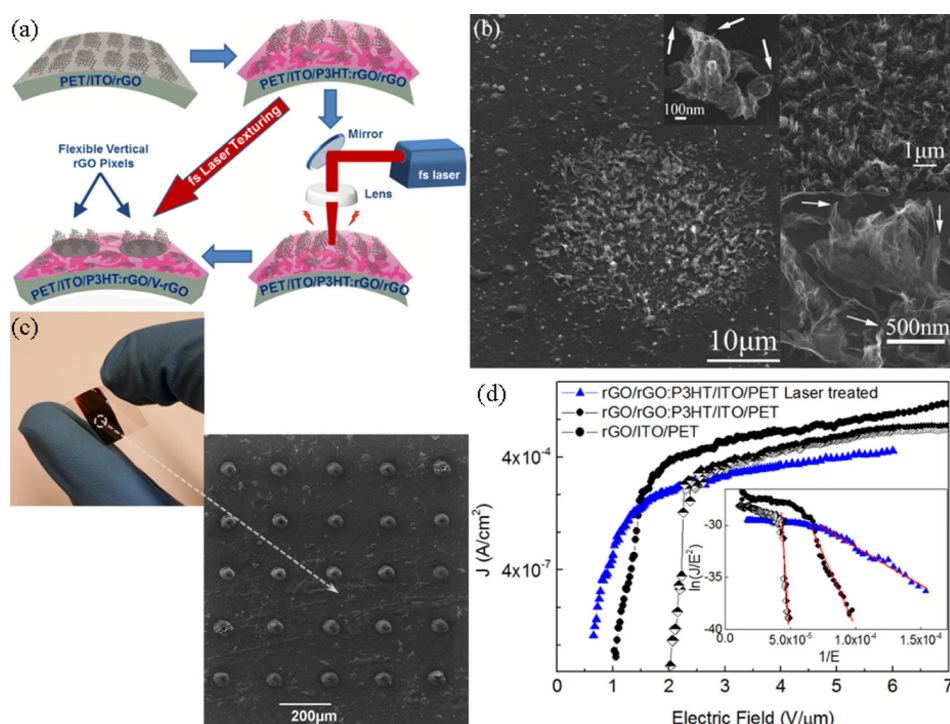


FIG. 2. (a) Schematic representation of the methodology developed for the fabrication of V-rGO field emission pixels; (b) FESEM views of a single pixel obtained via laser induced texturing of the top rGO layer. The insets depict typical views of the morphology of the textured rGO areas, while the arrows indicate sharp graphene edges exposed due to laser action; (c) Optical and FESEM view of a flexible V-rGO cathode comprising an array of emitting pixels, each of which consists of vertically oriented rGO sheets, fabricated by direct laser writing; (d) J - E FE characteristics of flexible laser fabricated V-rGO cathode compared to untreated and neat rGO ones. The inset presents the respective Fowler-Nordheim plots.

TABLE II. Field emission properties of rGO:P3HT and V-rGO:P3HT with 20 or 40 mm ROC. The \pm values denote the standard deviation of each measured or estimated quantity.

Sample	rGO:P3HT	rGO:P3HT ROC = 40 mm	V-rGO:P3HT	V-rGO:P3HT ROC = 40 mm	V-rGO:P3HT ROC = 20 mm
Turn-on field, F_{to} (V/ μ m)	1.0 ± 0.1	1.1 ± 0.1	0.6 ± 0.1	0.6 ± 0.1	0.6 ± 0.1
Threshold field, F_{th} (V/ μ m)	1.4 ± 0.1	1.6 ± 0.1	0.8 ± 0.1	0.8 ± 0.1	0.8 ± 0.1
Field enhancement, β	2507 ± 112	2107 ± 120	8900 ± 235	8606 ± 252	3950 ± 184

spots could operate as a pixel in a functional graphene based flexible FED. The achieved pixel size corresponds to a spatial resolution compatible to the current standards of the flat panel display industry, which is of the order of 100 μ m/pixel. Single spots of the order of tenths of microns could be also achieved with holographic techniques.

The J - E curve measured from the laser-textured V-rGO flexible cathode is shown in Figure 2(d) in comparison with those from the neat rGO one and the best cathode measured on the rGO:P3HT composite substrate, respectively. The corresponding FN plots are shown in the inset. Remarkably, as shown in Table II, the FE performance can be further improved in case of the laser-textured V-rGO flexible cathode. In particular, the threshold field, E_{th} , which we define as the macroscopic field where the emission current density becomes 10 μ A/cm², was as low as ~ 0.8 V/ μ m for the V-rGO cathode which is almost two times lower from that measured on the non-irradiated rGO/rGO:P3HT area and almost three times lower than that of the neat rGO layer deposited on the flexible substrate. More importantly, the enhancement factor increases by almost four times for the V-rGO cathode compared to that estimated for the untreated one, and almost twenty times lower than that of the neat rGO layer, reaching the outstanding value of 8900. The above results demonstrate the outstanding performance of the flexible V-rGO cathodes which is superior to that of the best rGO field emitters reported to date.^{16,22}

A critical requirement for a flexible electronic device is the preservation of its electrical performance under extensive mechanical deformation. It is hence important to measure the FE properties of our flexible V-rGO emitters under various bending conditions. For this purpose, an adjustable metallic fixture was utilized to bend the cathodes at different radii of curvatures (ROC). Figures 3(a) and 3(b) present the FE characteristics measured from the best rGO and V-rGO cathodes, convexly bent with 20 mm and 40 mm ROC. It is observed that both cathodes could be bent down to a 40 mm ROC without a significant change of FE characteristics. Besides this, the performance practically remains unaffected upon repetitive cycles of 40 mm ROC bending. These results indicate that our device formed a stable rGO:P3HT/rGO junction under bent conditions that is potentially useful for flexible electronics. It is also interesting to note that the characteristic knee in the high-field region of the J - E characteristics is absent when the laser treated cathode is bent. This may be attributed to the reduced emitter/substrate contact resistance. On the other hand when the ROC became 20 mm, we observed dramatic reduction on the enhancement factor, probably due to the mechanical damage of the effective aspect ratio of the emitting sharp edges. At the same time the turn on field value had no significant change, indicating that

the nature of the emitting sites is preserved upon bending; as a result, the local field needed to initiate emission per emitting site remains unaffected.

What should finally be mentioned is the remarkable stability of our flexible V-rGO cathodes under continuous operation. Indeed, it was observed (results not shown) that the emission current at constant voltage was remarkably stable for more than 30 h of continuous operation for both the untreated and laser treated cathodes. Additionally, the fluctuations of the emission current observed over the 30 h of operation were within $\pm 20\%$ of its initial value. Such fluctuations are commonly attributed to molecular adsorption and/or ion bombardment of the emitting sites by residual gases, the emission current under prolonged operation.

In conclusion, we have developed solution-processable, graphene-based, flexible FE cathodes via a direct laser texturing technique. The primary advantage of utilizing laser irradiation lies in the ability for *in-situ* controlled epidermal

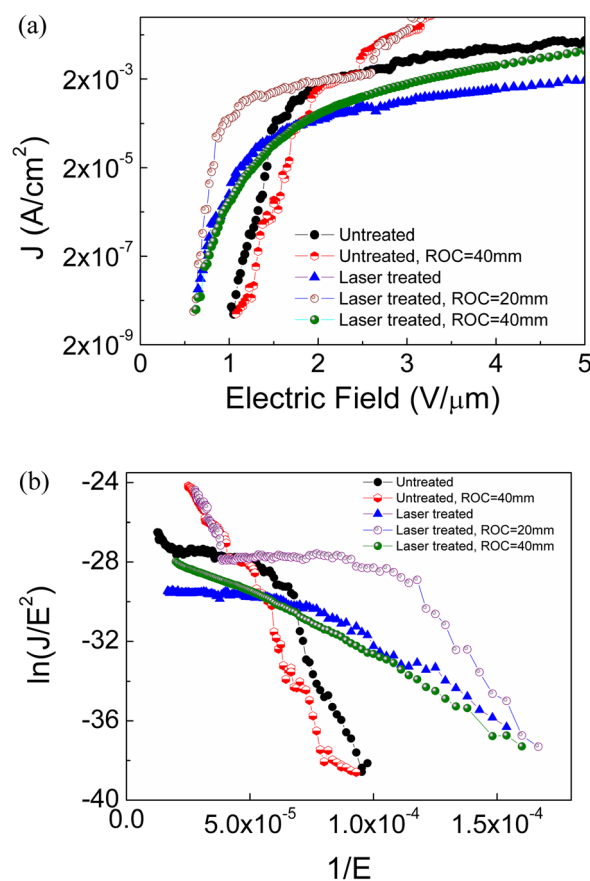


FIG. 3. (a) J - E FE characteristics of flexible rGO and V-rGO cathodes operating under bending at a 20 or 40 mm ROC. The respective J - E curves for devices operating without bending are also shown. (b) The respective Fowler-Nordheim plots of the FE characteristics shown in (a).

treatment that causes vertical alignment of rGO sheets and thus increased field enhancement, without practically affecting the integrity of the thermally sensitive substrate underneath. Our fabrication technique obviates the need for time-consuming and labor-intensive lithography, while no photomasks, or complex clean room operations are required. This work may pave the way for the potential use of laser treated graphene for applications related to FEDs and other flexible electronic devices.

This research has been co-financed by the European Union (European Social Fund–ESF) and Greek national funds through the Operational Program “Education and Lifelong Learning” of the National Strategic Reference Framework (NSRF)–Research Funding Program: ARCHIMEDES III. Investing in knowledge society through the European Social Fund.

- ¹K. Jain, M. Klosner, M. Zemel, and S. Raqhunandan, *Proc. IEEE* **93**, 1500–1510 (2005).
- ²T. Z. Kosc, “Particle display technologies become electronic paper,” *Optics and Photonics News*, 2005, pp. 18–25.
- ³Y. Guo, B. Wu, H. Liu, Y. Ma, Y. Yang, J. Zheng, G. Yu, and Y. Liu, *Adv. Mater.* **23**, 4626–4630 (2011).
- ⁴M. M. Stylianakis, E. Stratakis, E. Koudoumas, E. Kymakis, and S. H. Anastasiadis, *ACS Appl. Mater. Interfaces* **4**, 4864–4870 (2012).
- ⁵W. J. Yu, S. H. Chae, and S. Y. H. Lee, *Nano Lett.* **11**, 1344–1350 (2011).
- ⁶N. De Jong, Y. Lamy, K. Schoots, and T. H. Oosterkamp, *Nature* **420**, 393 (2002).
- ⁷K. B. K. Teo, E. Minoux, L. Hudanski, F. Peauger, J.-P. Schnell, L. Gangloff, P. Legagneux, D. Dieumegard, G. A. J. Amaratunga, and W. I. Milne, *Nature* **437**, 968 (2005).
- ⁸G. Z. Yue, Q. Qiu, B. Gao, Y. Cheng, J. Zhang, H. Shimoda, S. Chang, J. P. Lu, and O. Zhou, *Appl. Phys. Lett.* **81**, 355–357 (2002).
- ⁹L. F. Velasquez-Garcia, A. I. Akinwande, and M. Martinez-Sanchez, *J. Microelectromech. Syst.* **15**, 1272–1280 (2006).
- ¹⁰A. A. Fomani, A. I. Akinwande, and L. F. Velasquez-Garcia, *J. Phys. Conf. Ser.* **476**, 012014 (2013).
- ¹¹D. E. Engelsen, *Phys. Proc.* **1**, 355–365 (2008).
- ¹²D. A. Dikin, S. Stankovich, E. J. Zimney, R. D. Piner, G. H. B. Dommett, G. Evmenenko, S. T. Nguyen, and R. S. Ruoff, *Nature* **448**, 457 (2007).
- ¹³E. Stratakis, G. Eda, H. Yamaguchi, E. Kymakis, C. Fotakis, and M. Chhowalla, *Nanoscale* **4**, 3069–3074 (2012).
- ¹⁴S. Stankovich, D. A. Dikin, R. D. Piner, K. A. Kohlhaas, A. Kleinhammes, Y. Jia, Y. Wu, S. T. Nguyen, and R. S. Ruoff, *Carbon* **45**, 1558–1565 (2007).
- ¹⁵E. Kymakis, K. Savva, M. M. Stylianakis, C. Fotakis, and E. Stratakis, *Adv. Funct. Mater.* **23**, 2742–2749 (2013).
- ¹⁶H. Yamaguchi, K. Murakami, G. Eda, T. Fujita, P. Guan, W. Wang, C. Gong, J. Boisse, S. Miller, M. Acik *et al.*, *ACS Nano* **5**, 4945–4952 (2011).
- ¹⁷I. Lahiri, V. P. Verma, and W. Choi, *Carbon* **49**, 1614–1619 (2011).
- ¹⁸D. H. Lee, J. A. Lee, W. J. Lee, and S. O. Kim, *Small* **7**(1), 95–100 (2011).
- ¹⁹M. Arif1, H. Kwang, B. Y. Lee, J. Lee, D. H. Seo, S. Seo, J. Jian, and S. Hong, *Nanotechnology* **22**, 355709 (2011).
- ²⁰M. F. El-Kady and R. B. Kaner, *ACS Nano* **8**, 8725 (2014).
- ²¹G. Kakavelakis, D. Konios, E. Stratakis, and E. Kymakis, *Chem. Mater.* **26**, 5988 (2014).
- ²²G. Viskadourous, M. M. Stylianakis, E. Kymakis, and E. Stratakis, *ACS Appl. Mater. Interfaces* **6**(1), 388–393 (2013).
- ²³G. Viskadourous, A. Zak, M. Stylianakis, E. Kymakis, R. Tenne, and E. Stratakis, *Small* **10**, 2398 (2014).
- ²⁴M. Sveningsson, M. Jonsson, O. A. Nerushev, F. Rohmund, and E. E. B. Campbell, *Appl. Phys. Lett.* **81**, 1095 (2002).
- ²⁵A. T. H. Chuang, J. Robertson, B. O. Boskovic, and K. K. K. Koziol, *Appl. Phys. Lett.* **90**, 123107 (2007).
- ²⁶E. Minoux, O. Groening, K. B. K. Teo, S. H. Dalal, L. Gangloff, J. P. Schnell, L. Hudanski, I. Y. Y. Bu, P. Vincent, P. Legagneux, G. A. J. Amaratunga, and W. I. Milne, *Nano Lett.* **5**, 2135 (2005).
- ²⁷W. J. Zhao, W. Rochanachivapar, and M. Takai, *J. Vac. Sci. Technol. B* **22**, 1315–1318 (2004).
- ²⁸A. Modinos, *Field, Thermionic, and Secondary Electron Emission Spectroscopy* (Plenum, New York, 1984).
- ²⁹M. Qian, T. Feng, H. Ding, L. Lin, H. Li, Y. Chen, and Z. Sun, *Nanotechnology* **20**, 425702 (2009).
- ³⁰I. Alexandrou, E. Kymakis, and G. A. J. Amaratunga, *Appl. Phys. Lett.* **80**, 1435 (2002).